International Journal of Non-Linear Mechanics 78 (2016) 66–71

Contents lists available at ScienceDirect

International Journal of Non-Linear Mechanics

journal homepage: www.elsevier.com/locate/nlm

Dynamics of an oscillator with delay parametric excitation

Lauren Lazarus, Matthew Davidow, Richard Rand *

[a] Cornell University, Ithaca, NY, USA

ARTICLE INFO

Article history:
Received 3 July 2015
Received in revised form
13 October 2015
Accepted 14 October 2015
Available online 23 October 2015

Keywords:
Differential-delay equation
Parametric excitation
Limit cycle oscillator
Non-linear dynamics

ABSTRACT

This paper involves the dynamics of a delay limit cycle oscillator being driven by a time-varying perturbation in the delay:

$$\dot{x} = -x(t-T(t)) - \epsilon x^3$$

with delay $T(t) = \frac{\pi}{2} + \epsilon k + \epsilon \cos \omega t$. This delay is chosen to periodically cross the stability boundary for the $x=0$ equilibrium in the constant-delay system.

For most of parameter space, the system is non-resonant, leading to quasiperiodic behavior. However, a region of 2:1 resonance is shown to exist where the system's response frequency is entrained to half of the forcing frequency ω. By a combination of analytical and numerical methods, we find that the transition between quasiperiodic and entrained behavior consists of a variety of local and global bifurcations, with corresponding regions of multiple stable and unstable steady-states.

1. Introduction

A recent study [1] of dynamical systems with delayed terms has considered the following "delay limit cycle oscillator" in the form of a differential-delay equation (DDE):

$$\dot{x} = -x(t-T_0) - \epsilon x^3 \tag{1}$$

This system exhibits a supercritical Hopf bifurcation at delay $T_0 = \pi/2$ such that the equilibrium point at the origin $x=0$ is stable for $T_0 < \pi/2$ and unstable otherwise. The stable limit cycle for $T_0 > \pi/2$ is created with natural frequency 1 [2–4]. For an introduction to DDEs, see [5].

Eq. (1) with $\epsilon = 0$ has had application to insect locomotion [6].

This paper considers a system of the same form as Eq. (1), but with a periodically time-varying delay $T(t) = \pi/2 + \epsilon k + \epsilon \cos \omega t$:

$$\dot{x} = -x(t-T(t)) - \epsilon x^3 = -x\left(t - \frac{\pi}{2} - \epsilon k - \epsilon \cos \omega t\right) - \epsilon x^3 \tag{2}$$

The delay T is taken to be time-dependent such that the system may periodically cross the Hopf bifurcation exhibited by the constant T case. This causes the stability of the $x=0$ equilibrium to regularly alternate between stable and unstable. We would anticipate the equilibrium being stable if it is in the stable region for more than half of the forcing period, and unstable otherwise. However, we will show that the effect of this forcing may cause unexpected behavior due to resonance between the forcing frequency ω and the frequency of the limit cycle created in the Hopf.

The effect of time-periodic delay on an oscillator has been studied with application to turning processes with varying spindle speed in machine-cutting [7].

2. Non-resonant two-variable expansion

We begin by expanding the system about the $\epsilon = 0$ solution, using two time variables, fast time u and slow time v:

$$u = t \quad v = \epsilon t \quad x = x_0 + \epsilon x_1 + O(\epsilon^2) \tag{3}$$

The multiple time scales lead to the restatement of the derivative:

$$\dot{x} = \frac{dx}{dt} = \frac{\partial x}{\partial u}\frac{du}{dt} + \frac{\partial x}{\partial v}\frac{dv}{dt} = x_u + \epsilon x_v \tag{4}$$

The delay term is also approximated by its Taylor expansion:

$$x_d = x(u-T, v-\epsilon T) = x\left(u - \frac{\pi}{2}, v\right) - \epsilon(k + \cos \omega u)x_u\left(u - \frac{\pi}{2}, v\right) - \epsilon\frac{\pi}{2}x_v\left(u - \frac{\pi}{2}, v\right) + O(\epsilon^2) \tag{5}$$

Within the original equation with these expansions applied, we can find the coefficients of each power of ϵ. The O (1) terms ($\epsilon = 0$) give the differential equation:

$$x_{0u} + x_0\left(u - \frac{\pi}{2}, v\right) = 0 \tag{6}$$

* Corresponding author.
E-mail addresses: ll479@cornell.edu (L. Lazarus), mbd83@cornell.edu (M. Davidow), rhr2@cornell.edu (R. Rand).

http://dx.doi.org/10.1016/j.ijnonlinmec.2015.10.005
0020-7462/

with a solution of the form:

$$x_0(u,v) = A(v)\ \cos\ u + B(v)\ \sin\ u \tag{7}$$

The $O(\epsilon)$ terms are found from the original (expanded) equation to give an equation for x_1:

$$x_{1u} + x_1\left(u-\frac{\pi}{2},v\right) = -x_{0v} + (k+\ \cos\ \omega u)x_{0u}\left(u-\frac{\pi}{2},v\right) + \frac{\pi}{2}x_{0v}\left(u-\frac{\pi}{2},v\right) - x_0^3 \tag{8}$$

Since we will be looking to eliminate secular terms $\cos(u)$ and $\sin(u)$, at this point we note that some terms' resonance or non-resonance are dependent on the value of ω, in particular:

$$(\cos\ \omega u)(A\ \cos\ u + B\ \sin\ u) = \frac{A}{2}(\cos(\omega+1)u + \cos(\omega-1)u) + \frac{B}{2}(\sin(\omega+1)u - \sin(\omega-1)u) \tag{9}$$

Here we will split our analysis into two cases, resonant ($\omega \approx 2$) and non-resonant ($\omega \not\approx 2$), in order to account for the presence or absence of the resonant terms that arise from $\cos\ \omega u$.

2.1. Non-resonant behavior

Eliminating secular terms in the case where $\omega \not\approx 2$ results in the approximation and slow flow:

$$(2\pi^2+8)A' = 8kA - 4\pi kB + (3\pi B - 6A)(A^2+B^2) \tag{10}$$

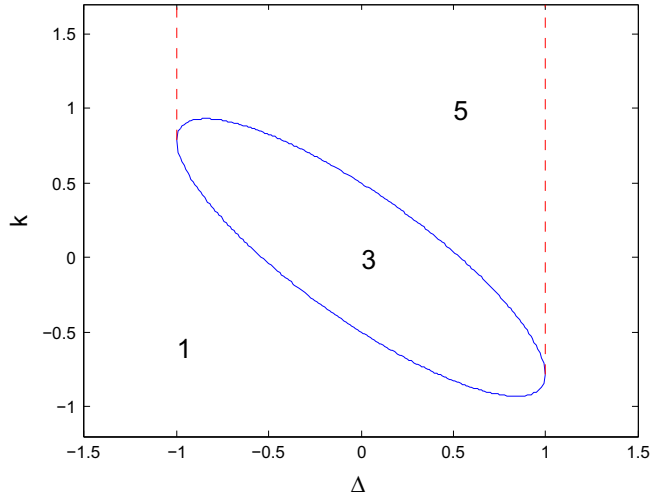

Fig. 1. Regions with 1, 3, and 5 slow flow equilibria, bounded by (dashed) double saddle-node bifurcations and (solid) pitchfork bifurcations.

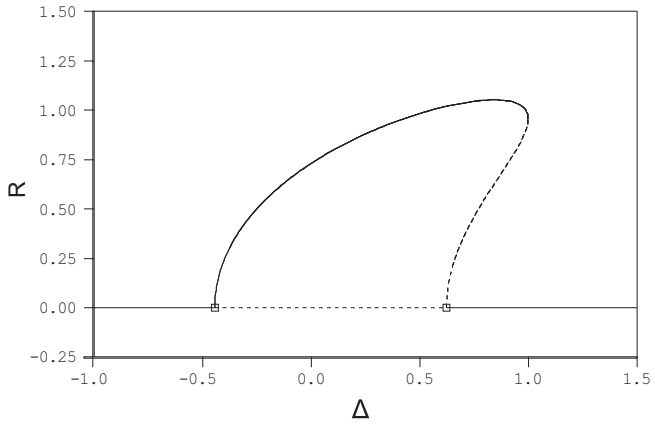

Fig. 2. AUTO results for $k=-0.1$ with varying Δ. Plotting the amplitude $R=\sqrt{A^2+B^2}$ of the $x(t)$ response for the equilibria, with stability information (solid is stable, dashed is unstable). All points on the $R\neq 0$ curve represent 2 equilibria by symmetry.

$$(2\pi^2+8)B' = 8kB + 4\pi kA - (3\pi A + 6B)(A^2+B^2) \tag{11}$$

Transforming to polar form by taking $A = R\ \cos\ \theta$ and $B = R\ \sin\ \theta$, to result in the new form $x_0(u,v) = R(v)\cos(u-\theta(v))$, gives:

$$(\pi^2+4)R' = R(4k-3R^2) \tag{12}$$

$$(2\pi^2+8)\theta' = \pi(4k-3R^2) \tag{13}$$

The R' equation is uncoupled, allowing us to study it separately. $R=0$ solves $R'=0$ for all parameter values (representing the origin $x=0$); this solution is stable for all $k<0$. For $k>0$ the stable solution is $R=4k/3$, with a corresponding $\theta'=0$. Based on this result, $x(t)$ is approximated to have response frequency 1 for $k>0$, as in the original limit cycle oscillator Eq. (1) with $T_0 > \pi/2$.

We note that in this expansion, the periodic forcing is shown to have no effect to this order. By expanding about the resonant forcing frequency $\omega = 2$ below, we will see that the second frequency does have an effect on the non-resonant behavior as well as behavior within the resonant region.

3. Resonant two-variable expansion

According to Eq. (9), the choice $\omega = 2$ makes the system resonant. To consider this behavior, we will redefine the two-variable expansion about this value by defining $\omega = 2+\epsilon\Delta$.

Using new variables for fast time ξ and slow time η to expand about the resonance at $\omega = 2$:

$$\omega t = 2\xi = 2(1+\epsilon\Delta/2)t \quad \eta = \epsilon t \tag{14}$$

$$\dot{x} = \frac{dx}{dt} = \frac{\partial x}{\partial \xi}\frac{d\xi}{dt} + \frac{\partial x}{\partial \eta}\frac{d\eta}{dt} = (1+\epsilon\Delta/2)x_\xi + \epsilon x_\eta \tag{15}$$

We proceed as before. The x_0 solution takes the same form as Eq. (7) in terms of the new time variables:

$$x_0(\xi,\eta) = A(\eta)\cos\ \xi + B(\eta)\sin\ \xi \tag{16}$$

while the $O(\epsilon)$ terms give the following equation for x_1:

$$x_{1\xi} + x_1\left(\xi-\frac{\pi}{2},\eta\right) = -x_{0\eta} - \frac{\Delta}{2}x_{0\xi} + \left(\frac{\pi\Delta}{4} + k + \cos\ 2\xi\right)x_{0\xi}\left(\xi-\frac{\pi}{2},\eta\right) + \frac{\pi}{2}x_{0\eta}\left(\xi-\frac{\pi}{2},\eta\right) - x_0^3 \tag{17}$$

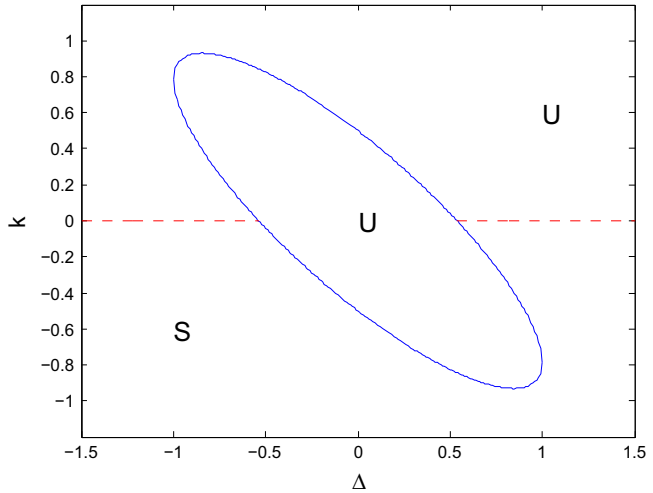

Fig. 3. Stability of $x=0$ near the resonance; "U" is unstable, "S" is stable. Changes in stability are caused by pitchfork bifurcations (solid line) and Hopf bifurcations (dashed line).

Within the resulting equation, we choose $A(\eta)$ and $B(\eta)$ to eliminate secular terms by collecting the coefficients of the $\sin(\xi)$ and $\cos(\xi)$ terms. This results in the following system of ordinary differential equations as the slow flow of the system:

$$(2\pi^2+8)A' = (8k+4)A+(2\pi-4\pi k-\pi^2\Delta-4\Delta)B+(-6A+3\pi B)(A^2+B^2) \quad (18)$$

$$(2\pi^2+8)B' = (2\pi+4\pi k+\pi^2\Delta+4\Delta)A+(8k-4)B+(-6B-3\pi A)(A^2+B^2) \quad (19)$$

where we have used $x_0(\xi-\pi/2,\eta) = -x_{0\xi}$ from the $O(1)$ terms to simplify the delay terms in Eq. (17). We note that Eqs. (18) and (19) are similar to the non-resonant slow flow Eqs. (10) and (11), but include additional terms caused by the resonance with the parametric forcing term.

This system of slow flow equations exhibits an assortment of bifurcation phenomena. Its steady-state solutions will include equilibrium points, representing periodic motions in $x(t)$, and limit cycles, corresponding to quasiperiodic behavior of the original system.

4. Slow flow equilibria

Equilibria in the slow flow solve $A' = B' = 0$. We use Maxima to eliminate B and obtain a single expression $f(A) = 0$, then additionally require $f'(A) = 0$ to find double roots in A, which will include pairs of equilibrium points coalescing in saddle-node bifurcations.

Eliminating A from these equations results in multiple expressions representing curves in $\Delta-k$ parameter space. The following locations in parameter space are observed to correspond to double roots in (A,B):

$$16k^2+8\pi\Delta k+(\pi^2+4)\Delta^2 = 4 \quad (20)$$

$$\Delta = \pm 1 \quad (21)$$

Eq. (20) is an ellipse which may be shown to represent a pair of pitchfork bifurcations off of $A = B = 0$. Eq. (21) represents double saddle-node bifurcations away from the origin, transitioning between regions of 1 and 5 equilibria; this restricts them to k values above the ellipse. Together these bifurcation curves describe regions in parameter space with 1, 3, and 5 slow flow equilibria, as can be seen in Fig. 1.

Results from AUTO bifurcation continuation software [8], used on the slow flow for $k = -0.1$ and varying Δ, show the interaction of the equilibria as the system crosses these bifurcation curves (see Fig. 2).

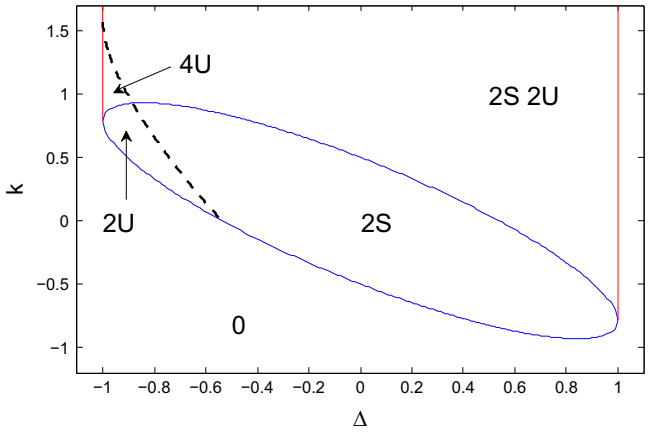

Fig. 4. Numbers of stable/unstable non-trivial equilibria (that is, besides $A = B = 0$). Ellipse is the set of pitchfork bifurcations (Eq. (20)). Vertical lines are double saddle-node bifurcations (Eq. (21)). The dashed curve is a Hopf bifurcation (Eq. (28)).

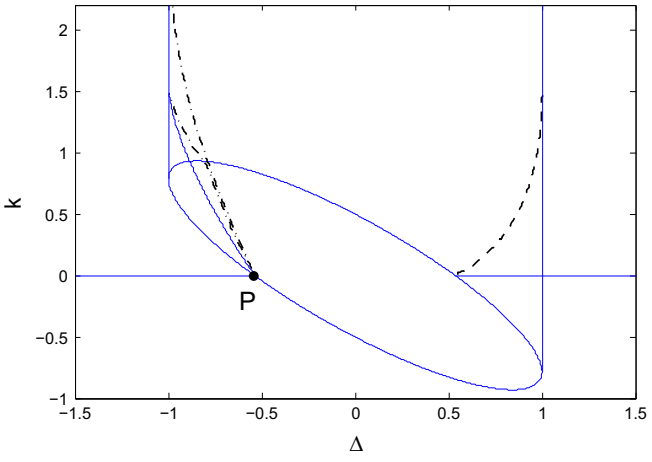

Fig. 5. Local bifurcation curves (solid lines) as seen in Figs. 3 and 4. Global bifurcation curves (dashed lines) found numerically. Degenerate point P also marked, see Fig. 8.

5. Stability of $x=0$

The stability of the $x=0$ solution is governed by the Jacobian matrix J for the slow flow about $A = B = 0$:

$$J = \begin{bmatrix} 8k+4 & 2\pi-4\pi k-(\pi^2+4)\Delta \\ 2\pi+4\pi k+(\pi^2+4)\Delta & 8k-4 \end{bmatrix} \quad (22)$$

Since the eigenvalues λ of J satisfy the characteristic equation:

$$\lambda^2-\mathrm{tr}(J)\lambda+\det(J) = 0 \quad (23)$$

the condition for stability $\mathrm{Re}(\lambda) < 0$ requires both $\det(J) > 0$ and $\mathrm{tr}(J) < 0$ [9].

The stability boundary $\det(J) = 0$ gives Eq. (20) and corresponds to the ellipse in Fig. 1. The inside of the ellipse gives $\det(J) < 0$ such that the origin is a saddle point and therefore unstable.

Outside the ellipse where $\det(J) > 0$, the stability of the origin depends on the sign of $\mathrm{tr}(J) = 16k$. At the stability boundary $\mathrm{tr}(J) = 0$, the eigenvalues λ are purely imaginary leading to a Hopf bifurcation. Thus the origin $A = B = 0$ undergoes a Hopf bifurcation at $k=0$ under the condition which restricts to the outside of the ellipse:

$$\Delta^2 > 1/(\pi^2+4) \quad (24)$$

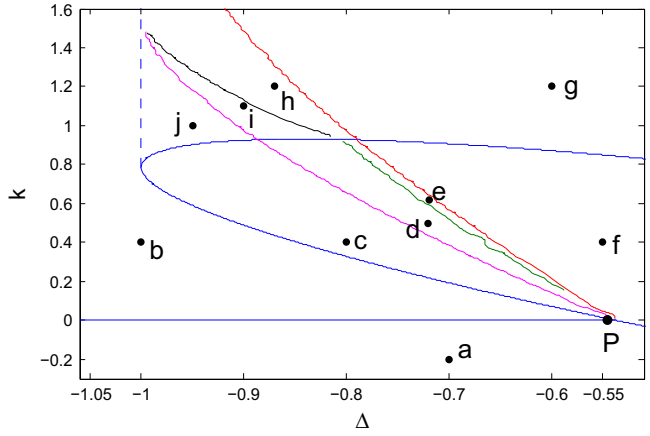

Fig. 6. Zoom of Fig. 5 with labeled points explored in Figs. 7 and 8.

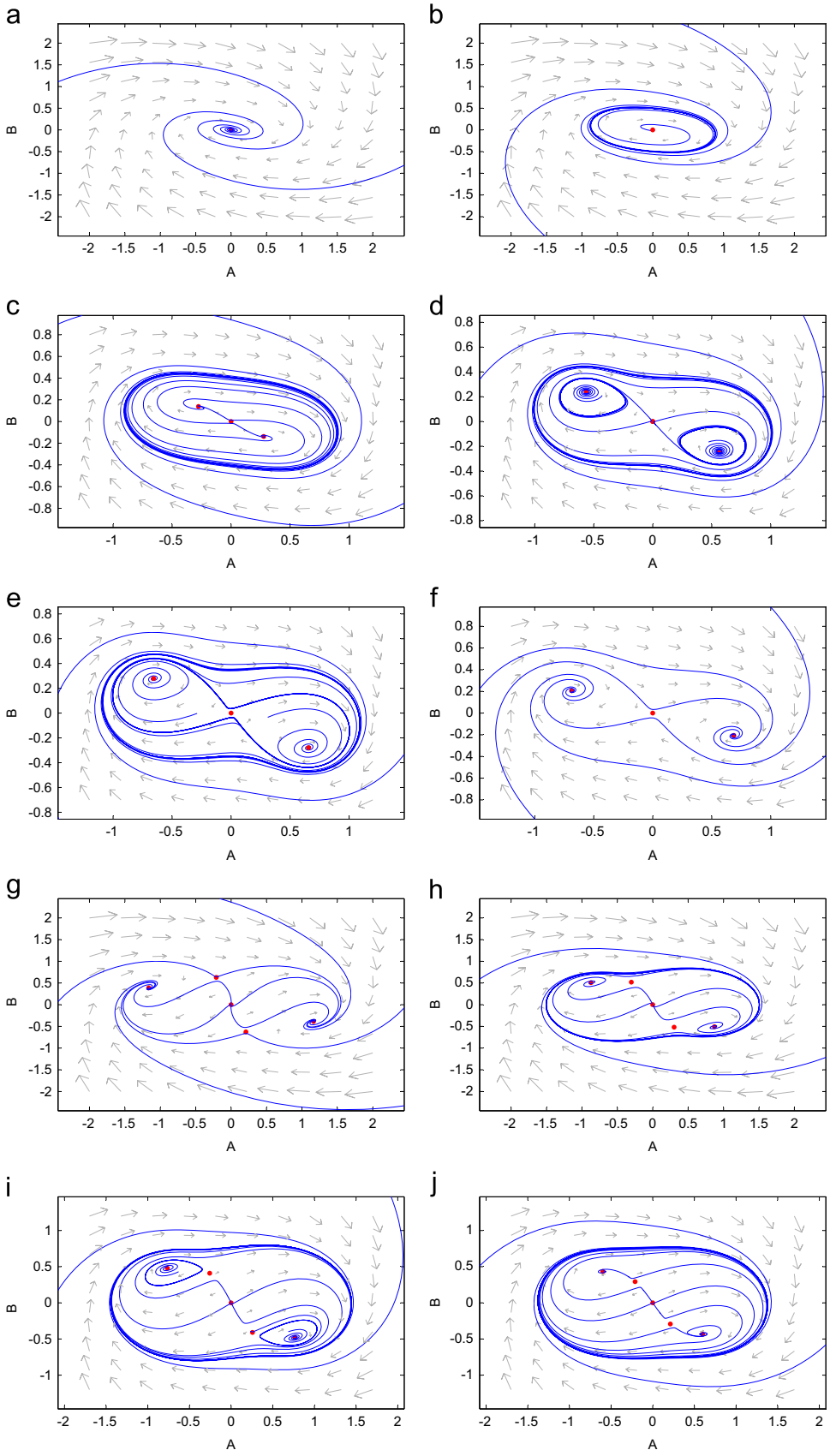

Fig. 7. Representative phase portraits of the slow flow from each region of parameter space, locations as marked in Fig. 6. Obtained with numerical integration via `pplane`.

At the Hopf bifurcation, the eigenvalues $\lambda = iW$ give the response frequency to be:

$$W = \sqrt{(\pi^2+4)^2\Delta^2 - 4(\pi^2+4)} \tag{25}$$

in slow time η, or frequency ϵW in t.

These conditions on the determinant and trace, together with the corresponding pitchfork and Hopf bifurcation curves, lead to the stability regions seen in Fig. 3.

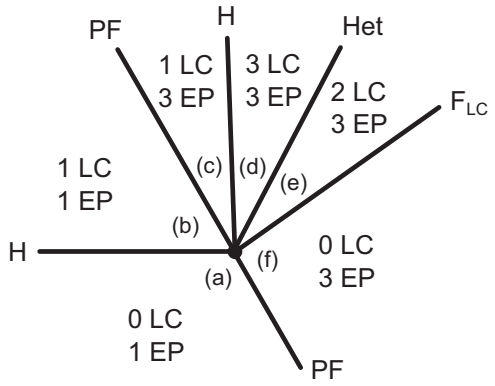

Fig. 8. Schematic at degenerate point P from Figs. 5 and 6, showing the number of limit cycles (LC) and equilibrium points (EP) in each labeled region. Bifurcation types also shown: Hopf (H), pitchfork (PF), heteroclinic (Het), and limit cycle fold (F_{LC}).

6. The limit cycle from $k=0$ Hopf

The Hopf bifurcation off the origin at $k=0$ is found to be supercritical, resulting in a stable limit cycle in the slow flow for $k>0$ for values of Δ satisfying Eq. (24), i.e. outside the ellipse. This limit cycle represents a quasiperiodic motion in the overall system, on account of the two frequencies represented: the original Hopf frequency ϵW and the halved forcing frequency $\omega/2 = 1+\epsilon\Delta/2$.

We will show that this limit cycle is destroyed as the system parameters move into the resonance region (i.e. as $\omega \to 2$ or $\Delta \to 0$).

7. Stability of $x \neq 0$ slow flow equilibria

Just as for the $A=B=0$ equilibrium above, we consider the linear stability of the non-trivial equilibria of the slow flow by linearizing about their locations [9]. The pair of equilibria found in both the regions of 3 and 5 equilibria (see Fig. 1) have the locations:

$$A_m = \pm\sqrt{\left(\frac{2k}{3}+\frac{\pi\Delta}{6}+\frac{1}{3}\right)\left(1+\sqrt{1-\Delta^2}\right)-\frac{\Delta^2}{3}} \tag{26}$$

$$B_m = \mp\sqrt{\left(\frac{2k}{3}+\frac{\pi\Delta}{6}-\frac{1}{3}\right)\left(1-\sqrt{1-\Delta^2}\right)+\frac{\Delta^2}{3}} \tag{27}$$

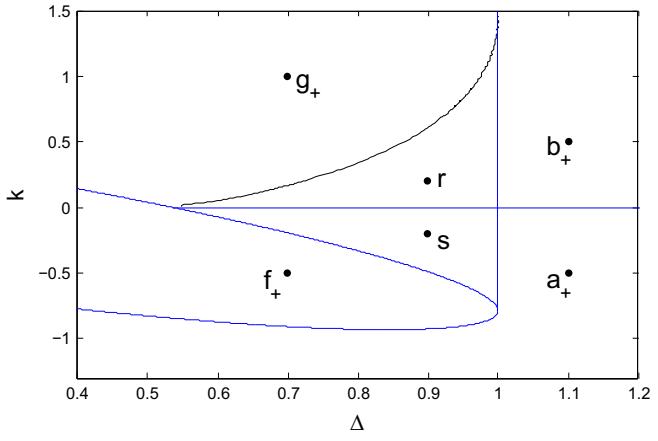

Fig. 9. Zoom of Fig. 5 with labeled points. Points a_+, b_+, f_+, and g_+ are qualitatively identical to points a, b, f, and g respectively from Fig. 6.

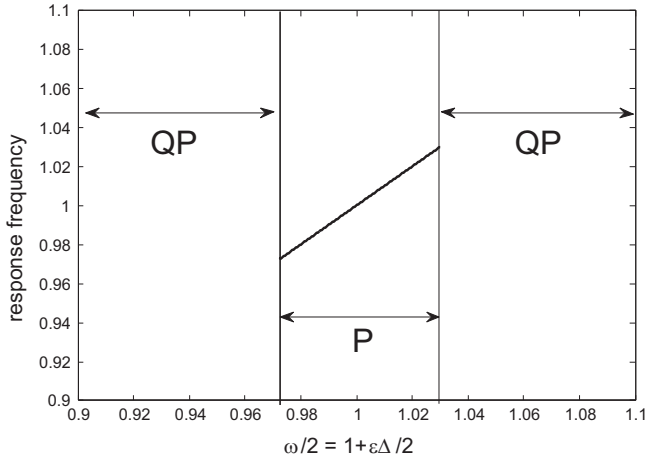

Fig. 11. The system is entrained to periodic motion (P) at frequency $\omega/2$ within the resonance region (shown for $k=0.05$). It exhibits quasiperiodic motion (QP) with multiple frequencies everywhere else.

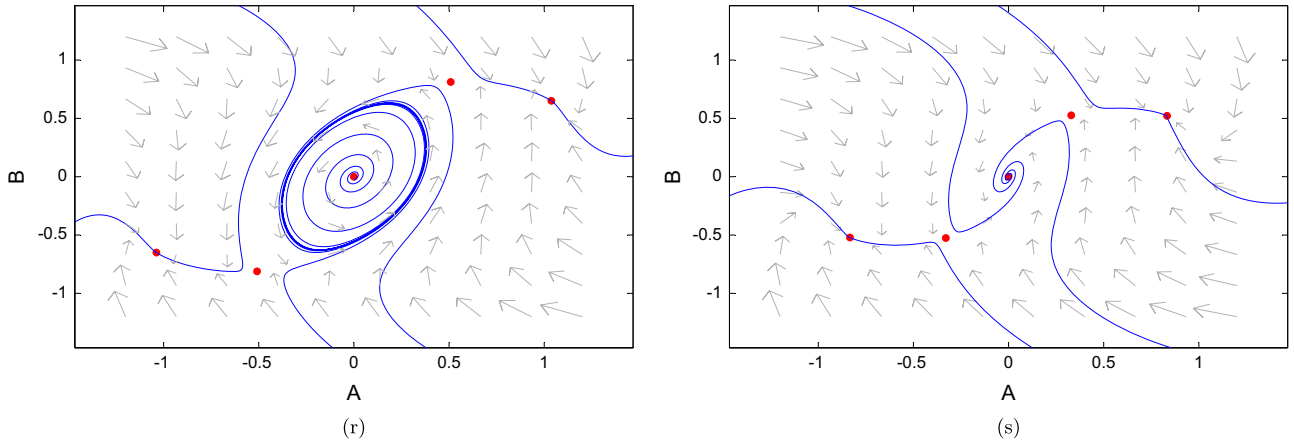

Fig. 10. Representative phase portraits of the slow flow from regions of parameter space, locations as marked in Fig. 9. Obtained with numerical integration via `pplane`.

By linearizing about this location and looking for pure imaginary eigenvalues, we find that these equilibria change stability in Hopf bifurcations on the curve:

$$k = -\sqrt{1-\Delta^2} - \frac{\pi\Delta}{2} \tag{28}$$

This curve intersects with the ellipse when $k=0$ and therefore only exists for $k>0$. It reaches an end by approaching $\Delta=-1$ tangentially as k approaches $\pi/2$.

In contrast, the pair of equilibria which exist only in the region of 5 equilibria (see Fig. 1):

$$A_p = \pm\sqrt{\left(\frac{2k}{3}+\frac{\pi\Delta}{6}+\frac{1}{3}\right)\left(1-\sqrt{1-\Delta^2}\right)-\frac{\Delta^2}{3}} \tag{29}$$

$$B_p = \mp\sqrt{\left(\frac{2k}{3}+\frac{\pi\Delta}{6}-\frac{1}{3}\right)\left(1+\sqrt{1-\Delta^2}\right)+\frac{\Delta^2}{3}} \tag{30}$$

are found to be unstable saddle points wherever they exist.

The foregoing discussion of stability of the non-trivial equilibria is summarized in Fig. 4.

8. Slow flow phase portraits

So far we have considered local bifurcations (pitchfork, saddle-node, Hopf) as seen in Figs. 3 and 4. Fig. 5 shows these bifurcations along with the global bifurcations that we will now discuss, being limit cycle folds and heteroclinic bifurcations.

We use Matlab to plot numerically obtained phase portraits of the slow flow Eqs. (18) and (19). Fig. 6 is a zoom of the left half of Fig. 5 with regions labeled corresponding to phase portraits in Fig. 7. Fig. 8 shows a schematic of the bifurcation curves in the neighborhood of point P.

Fig. 9 is a zoom of the right half of Fig. 5 with regions labeled corresponding to phase portraits in Fig. 10.

9. Stable motions of Eq. (2)

The previous figures (Figs. 1–10) correspond to the behaviors of the slow flow equations (18) and (19). Now we summarize the corresponding stable motions $x(t)$ in the original system Eq. (2). (Unstable motions are not mentioned since they will not be seen in simulations.)

- Region *a*: origin only, $x=0$ (no oscillation)
- Regions *f*, *g*: entrained motion only
- Region *b*, *c*, *j*: quasiperiodic (unentrained) motion only
- Regions *d*, *e*, *h*, *i*, *r*: quasiperiodic and entrained motions
- Region *s*: origin $x=0$ (no oscillation) and entrained oscillation

We note that in the regions with multiple stable solutions, the basins of attraction for each stable behavior are defined by initial conditions which are functions of time.

10. Conclusions

In this work, we considered the dynamics of a delay limit cycle oscillator whose delay is varied periodically across a critical value of the delay corresponding to a Hopf bifurcation, such that the equilibrium solution $x=0$ alternates in time between being stable and unstable.

For most forcing frequencies of the delay, the equilibrium at the origin $x=0$ is stable provided the average delay is smaller than the critical delay. If the average delay is larger than the critical delay, the system exhibits quasiperiodic behavior due to the coappearance of oscillations at the forcing-frequency along with oscillations at the limit cycle frequency.

However, the system has a 2:1 resonance which results in a small region of parameter space about $\omega=2$ where the oscillator behaves periodically. Within this region, the system is entrained to oscillate at half of the forcing frequency, see Fig. 11. We conjecture that other resonances (m:n) exist in this problem just as they do in Mathieu's equation [2], but we have not found them analytically or numerically as yet.

Within the transition between resonance and non-resonance, the system is found to have regions of multiple stable behaviors (periodic and quasiperiodic motions). Each steady-state has its own basin of attraction, and the long-term behavior is then determined by the initial conditions on $x(t)$. (These initial conditions consist of functions of time for a differential-delay equation.)

This system represents a particular form of parametric excitation which has been previously unstudied, where the periodic forcing term appears in the delay. A remarkably similar bifurcation set has been observed in a system which did not involve delay [10]. The system in [10] involved a second-order differential equation undergoing a Hopf bifurcation which was being forced parametrically.

References

[1] L. Lazarus, M. Davidow, R. Rand, Dynamics of a delay limit cycle oscillator with self-feedback, Nonlinear Dyn. 82 (2015) 481–488.

[2] R.H. Rand, Lecture Notes in Nonlinear Vibrations Published, First University Press, Ithaca, NY, online by the Internet, http://ecommons.library.cornell.edu/handle/1813/28989, 2012.

[3] R. Rand, Differential-delay equations, in: A.C.J. Luo, J.-Q. Sun (Eds.), Complex Systems: Fractionality, Time-delay and Synchronization, Springer, Berlin, 2011, pp. 83–117 (Chapter 3).

[4] S.L. Das, A. Chatterjee, Multiple scales without center manifold reductions for delay differential equations near Hopf bifurcations, Nonlinear Dyn. 30 (2002) 323–335.

[5] G. Stepan, Retarded Dynamical Systems: Stability and Characteristic Functions, Longman Scientific and Technical, Essex, England, 1989.

[6] A.F. Haselsteiner, C. Gilbert, Z.J. Wang, Tiger beetles pursue prey using a proportional control law with a delay of one half-stride, J. R. Soc. Interface 11 (2014).

[7] T. Insperger, G. Stepan, Stability analysis of turning with periodic spindle speed modulation via semidiscretization, J. Vib. Control 10 (2004) 1835–1855.

[8] E. Doedel, A. Champneys, T. Fairgrieve, Y. Kuznetsov, B. Sandstede, X. Wang, AUTO 97: Continuation and Bifurcation Software for Ordinary Differential Equations, 1998.

[9] J. Guckenheimer, P. Holmes, Nonlinear Oscillations, Dynamical Systems, and Bifurcations of Vector Fields, Springer-Verlag, New York, 1983.

[10] R. Rand, A. Barcilon, M. Morrison, Parametric resonance of Hopf bifurcation, Nonlinear Dyn. 39 (2005) 411–421.